Cellular and Molecular Bioengineering (2024) 17:229–241
https://doi.org/10.1007/s12195-024-00804-3

BMES BIOMEDICAL ENGINEERING SOCIETY

ORIGINAL ARTICLE

A Label-Free Colorimetric AuNP-Aptasensor for the Rapid Detection of *Vibrio cholerae O139*

Masilamani Karthikeyan[1] · **Pasupathi Rathinasabapathi**[1]

Received: 19 December 2023 / Accepted: 28 May 2024 / Published online: 14 June 2024

Abstract

Purpose Waterborne pathogens pose a significant threat to public health, emphasizing the continuous necessity for advancing robust detection techniques, particularly in preventing outbreaks associated with these pathogens. This study focuses on cholera, an infectious disease caused by *Vibrio cholerae*, serogroups O1 and O139, often transmitted through contaminated water and food, raising significant public health concerns in areas with poor sanitation and limited access to clean water.

Methods We developed a colorimetric biosensor using aptamer-functionalized gold nanoparticles to identify *Vibrio cholerae* O139 and address this issue. The detection mechanism relies on the color change of gold nanoparticles (AuNPs) from red to blue-purple induced by NaCl after the pathogen incubation and aptamer-target binding. Initial steps involved synthesizing and characterizing AuNPs, then exploring the impact of aptamer and NaCl concentrations on AuNP agglomeration. Optimization procedures for aptamer concentration and salt addition identified the optimal conditions for detection as 120 pM aptamers and 1 M NaCl.

Results The aptasensor demonstrated a robust linear relationship, detecting *V. cholerae* concentrations from 10^3 to 10^8 CFU/mL, with a limit of detection (LOD) of 587 CFU/mL. Specificity tests and accurate sample analyses confirmed the efficiency of the AuNPs aptasensor, showcasing its reliability and speed compared to traditional culture examination methods. Moreover, we extended the aptasensor to a paper-based sensing platform with similar detection principles.

Conclusion The change in color upon target binding was captured with a smartphone and analyzed using image processing software. The paper-based device detected the target in less than 2 min, demonstrating its convenience for on-field applications.

Keywords Aptasensor · *Vibrio cholera* · Colorimetric detection · Biosensor · AuNP · Paper-based detection

Introduction

Cholera, an acute intestinal disease caused by the Gram-negative bacterium *Vibrio cholerae*, remains a major global health concern [1]. This pathogen predominantly exists in two serogroups, O1 and O139, and thrives in aquatic environments. Cholera is primarily transmitted through consuming contaminated food and water, mainly via the fecal-oral route. Its devastating impact on public health is most pronounced in emerging and underdeveloped nations, where inadequate sanitation, lack of access to clean water, and poor hygiene practices prevail [2]. From 2009 to 2017, two-thirds of the cholera outbreaks reported in India were antibiotic-resistant, totaling 559 outbreaks [3]. To control and prevent cholera, health agencies worldwide have implemented various measures. However, there is an urgent need to develop cost-effective biosensing agents that are sensitive and rapid. High-risk cholera populations are often from lower socioeconomic backgrounds.

Cholera diagnosis traditionally relies on culture-based methods, considered as the gold standard for detection [4]. However, this method suffers from limitations in processing time and labor intensiveness. Several alternative techniques

Associate Editor Mehdi Nikkhah oversaw the review of this article.

✉ Pasupathi Rathinasabapathi
rathinap1@srmist.edu.in

Masilamani Karthikeyan
km1966@srmist.edu.in

[1] Department of Genetic Engineering, SRM Institute of Science and Technology, Kattankulathur, Tamil Nadu 603 203, India

have been explored, including gel electrophoresis [5], lateral flow immunoassays [6], and enzyme-linked immunosorbent assays (ELISA) [7]. In recent years, nucleic acid amplification testing methods like polymerase chain reaction (PCR) [8], loop-mediated isothermal amplification (LAMP) [9], and molecular rapid diagnostic tests (mRDTs) detected the cholera toxin genes [10]. However, the need for complex equipment, high operational costs, extended detection times, and the requirement for highly trained personnel pose significant challenges to these molecular techniques.

Aptamers are molecules used for detecting targets with a high degree of specificity and they are more stable, tailored at ease, and withstand temperature fluctuations compared to the antibodies used in traditional methods [11]. They are essentially single-stranded DNA or RNA molecules that are about the length of 35–100 nucleotides [12]. In whole cell-SELEX, live cells are used as targets to select aptamers that can bind specifically to the cell surface or internal components of the target cell. Therefore, aptamers can attach to their target materials through receptor-like action, and their high affinity and specificity make them useful in microbial detection [13].

Gold nanoparticles (AuNPs) exhibit a variety of colors in aqueous solution, and their absorption peaks typically fall within 500–550 nm [14]. Plasmonic nanoparticles, especially AuNPs have high surface plasmon resonance (SPR) and extinction coefficients in the visible spectrum. As a result, they are widely researched for their application in colorimetric sensing [15]. Colorimetric assays detect target analytes by monitoring material color changes, enabling quick on-site analysis [16]. Unlike traditional detection methods that require extensive preparation, complex methodologies, and skilled analysts, AuNP-based colorimetric assays are preferred for their ease of use, affordability, and portability in on-field studies. Nowadays, biosensors have gained prominence in disease detection because they can identify targets, and transduce interactions into measurable signals [17, 18]. Researchers discovered that nanoparticles conjugated with aptamers can create colorimetric aptasensors those sensors are used for visual recognition of microorganisms such as *Salmonella typhimurium* [19], *Vibrio parahaemolyticus* [20], *E. coli* O157: H7 [21], *Staphylococcus aureus* [22], *S. enteritidis* (Bayraç et al., 2017) [23], *Campylobacter jejuni* [24], *C. coli* [25], and *Listeria monocytogenes* [26]. Although colorimetric detection methods have been around for years, there are still no reported uses of aptasensors for detecting *V. cholerae* O139 [27].

In this method, the surface-conjugated aptamer protects the AuNPs from salt-induced aggregation. Upon the addition of the target, due to their higher affinity, the surface oligonucleotides effectively relocated toward their target, resulting in AuNPs aggregation. This aggregation reaction led to a noticeable color shift that could be seen with the naked eye [28]. Bioconjugates involving gold nanoparticles (AuNPs), encompassing antibodies, proteins, and oligonucleotides, have emerged as promising alternatives in diagnostic methods [29]. Researchers have expressed a keen interest in exploring the potential of aptamers conjugated with AuNPs (Apt-AuNPs) as biosensors for identifying diverse biological substances. Apt-AuNPs stand out as ideal platforms for optical sensing, facilitating applications in electrochemical, colorimetric, and fluorometric sensing.

However, prior studies on the use of AuNPs for colorimetric sensing of diverse materials have primarily focused on the color changes of AuNPs in the colloidal solution or in the solution phase, which are vulnerable to unfavorable aggregation due to their high reactivity [30]. A viable solution to this problem is to incorporate AuNPs onto a solid support, such as a polymer fiber [31], functionalized clay [32], or cellulose-based papers [33]. There is a growing demand for environmentally sustainable materials for biosensors and on-field detection devices, which has increased interest in using paper and its composites. Paper is abundant, mechanically stable, biodegradable, affordable, sustainable, and has many applications [34]. Paper-based sensors are particularly promising as they can be portable, simple, and fast detection tools, even with small sample volumes and minimal instrumentation. This will result in an AuNP-based solid sensor. For on-site sensing applications, immobilizing AuNPs on solid supports has increased stability, recyclability, and ease in transportation. Hence, we developed a colorimetric detection system for *V. cholerae* O139 using aptamers and gold nanoparticles (AuNPs). To achieve this, we conjugated *V. cholerae* O139-specific aptamers on the surface of AuNPs and coated them on Whatman filter paper discs. The result was a paper-based aptasensor that could detect *Vibrio cholerae* O139.

Materials and Methods

Materials and Instruments

A custom-synthesized whole-cell aptamer specific to *V. cholerae* O139 was obtained from Eurofins BPT Pvt Ltd in Chennai, India (data not shown). The *Vibrio cholerae* O139 strain was procured from the Microbial Type Culture Collection Centre (MTCC) in Chandigarh, India. Chemicals such as tri-sodium citrate ($Na_3C_6H_5O_7$), chloroauric acid ($HAuCl_4$), sodium chloride (NaCl), and Whatman filter paper Grade-I was purchased from HiMedia Pvt Ltd in Chennai, India. All chemicals were prepared using double autoclaved distilled water (ddH_2O). Transmission electron microscopy (TEM) images were obtained from JEM-2100 using JEOL, Japan equipment. The zeta particle sizer (Litesizer 500, Austria) was used to measure the charge and

size of AuNPs. The UV–vis spectrum was obtained using a GENESYS spectrophotometer (Thermo Fisher Scientific, USA). Photographs were taken using an iPhone 12 Pro Max.

Preparation and Characterization of Gold Nanoparticles (AuNPs)

Gold nanoparticles (AuNPs) were synthesized using a method established in a previous study [35]. In brief, a solution containing 0.3 mM $HAuCl_4$ was heated and stirred until it reached boiling point. Then 68 mM of $Na_3C_6H5O_7$ solution was added dropwise, and the mixture was heated for 30 min. The resulting solution had a wine-red color and was filtered through ultrafiltration membranes with a pore size of 0.22 µm stored at 4 °C until further use. The extinction coefficient of 2.7×10^8/M/cm was used for 20 nm-sized AuNP [36]. The concentration of AuNP was calculated using the Beer–Lambert law as follows: $Abosrbance_{520} = Extinction\ coefficient \times pathlength \times concentration$, whereas the path length is one centimeter and absorbance was measured at 520 nm. The concentration of synthesized AuNP was 0.24 mg/mL by using the above-mentioned method. Morphological characterization of AuNPs, evenly dispersed and salt-aggregated, was performed using a transmission electron microscope (TEM). TEM samples were prepared by placing colloidal solutions on carbon-coated copper imaging grids and allowing them to dry at room temperature.

Aptamer-Modified AuNP (Apt-AuNP) Preparation

AuNPs modified with aptamers were developed based on previous research [37]. The aptamer sequences were added to the AuNPs solution and incubated at different temperatures and intervals. After that, the AuNP and aptamer mixture complexes were centrifuged for 20 min at 8000×*g* at 4 °C to eliminate any unbound aptamers. The resulting pellet, which contained aptasensors conjugated with aptamers, was resuspended in ultra-pure water. The solution was analyzed using a UV–visible spectrophotometer to confirm the binding of aptamers. Finally, the aptamer-AuNP was stored in the dark at 4 °C until further use.

Optimization of Aptamer Sequence and NaCl Concentration

To determine the optimal concentration of NaCl that induces AuNP (gold nanoparticles aggregation), various concentrations of NaCl (0.5, 0.75, 1 M, 1.25 M, 1.5 M) were added to the aptasensor. The color changes were then observed. The ideal ratio of aptamers to AuNPs to maintain aptasensor stability in the presence of NaCl without *V. cholerae* O139 was evaluated by adding different concentrations of aptamers (ranging from 10 to 200 pM) to AuNPs in a 1:4 ratio. The mixture was then incubated at 37 °C for 5 min and centrifuged at 5000×*g* for 5 min to separate unbound aptamers. The resulting brick-red pellet was gently resuspended in double-distilled water. The AuNP-aptamer conjugates were added to a 96-well plate, and 1 M NaCl was added to each well. The color changes were observed, and UV–vis spectra were recorded. The absorption ratio (A_{720}/A_{520}) of AuNP–aptamer conjugates was determined using different NaCl and aptamer concentration combinations.

Sensitivity and Selectivity of Developed Biosensor

The sensitivity of the aptasensor was tested by using varying concentrations of *V. cholerae* O139 cells. The cells were obtained through serial dilution ranging from 1×10^1 to 1×10^8 CFU/mL. To test the specificity of the aptasensor, five different bacterial strains, namely *V. cholera O139*, *V. parahaemolyticus*, *S. aureus*, *A. hydrophila*, and *E. coli*, were individually evaluated. The bacterial cells were washed, resuspended, and adjusted to a concentration of 10^5 CFU/mL. The aptasensor was then incubated with each bacterial sample at 37 °C for 5 min. After this, 1 M NaCl was added, and any color changes and UV–vis spectra were recorded.

Vibrio cholerae O139 Detection in Environmental Samples

Vibrio cholerae O139 detection in environmental water bodies was done using the developed colorimetric sensor. A microporous layer with a pore size of 0.45 µm was used to filter out the macro residues in the water samples. The treated water samples were mixed with Tris–HCl buffer (10 mM, pH 7.5) in a ratio of 1:9 (v/v) [38]. Varying concentrations of *V. cholera* (ranging from 0 to 5×10^4 CFU/mL) were added to the samples, which were then monitored for colorimetric detection of *V. cholera*.

Fabrication of Aptasensor in Paper-Based Platform

A paper-based platform was designed to detect *V. cholera* O139 using aptasensor-modified Whatman filter paper (WFP) discs. To prepare the WFP discs, a clean puncher was used to create 1 cm diameter discs, which were then cleaned with deionized water, air-dried at room temperature, soaked in absolute ethanol for 1 h, and air-dried again at 60 °C [39]. A transparent adhesive sticky tape created a hydrophobic layer to prevent fluid flow influence (FFI) [40]. An optimal volume of aptasensor was added to the center of each disc and allowed to dry at room temperature. To detect *V. cholera*, the discs containing the aptasensor were incubated at 37 °C for 5 min with 10^7 *V. cholerae* O139 cells. Afterward,

1 M NaCl was added and incubated at 37 °C for 5 min, and any color changes in the discs were observed.

Results and Discussion

Principle of Aptasensor Detection Mechanism

The fundamental principles behind the colorimetric detection of *V. cholerae* O139 employing AuNPs are illustrated in (Fig. 1). AuNPs exhibit a vibrant ruby-red hue characteristic when they are dispersed with an interparticle distance that is regulated by negatively charged citrate ions [41]. Upon the introduction of NaCl, the initially dispersed AuNPs tend to aggregate, resulting in a conspicuous shift in color towards purple. This aggregation occurs because the Na^+ ions reduce the interparticle distance between AuNPs by neutralizing the negative charges of citrate ions. This, in turn, fosters electrostatic interactions among the particles, leading to observable changes in both the color and the surface plasmon wavelength of the AuNPs [42, 43]. The binding of target-specific aptamers to the surface of AuNPs forms an electric double layer that offers stability to the AuNPs against extensive NaCl-induced aggregation. As a result, even at elevated NaCl concentrations, the solution retains its characteristic ruby-red hue. However, in the presence of *V. cholerae* O139, the aptamers detach from the AuNPs and bind to the *V. cholerae* O139 cells owing to their higher affinity towards the target. Consequently, the unprotected AuNPs become susceptible to salt-induced aggregation.

Development of the Aptamer-Modified AuNP (Apt-AuNP)

The TEM images of the synthesized AuNPs revealed a high degree of uniformity, with an approximate average size of 17 nm. TEM images confirmed that AuNPs are generally spherical and monodispersed. However, the NaCl-triggered aggregation of AuNPs increases its size, but the aptamer-bounded AuNPs remain in their naturally dispersed state despite the addition of NaCl. The addition of target cells enhanced the aptamer dislocation from the AuNPs leaving them vulnerable to NaCl-induced aggregation (Fig. 2A) and a size distribution plot was plotted using DLS (Fig 2B). The shift in the SPR absorption spectrum of AuNPs from 520 nm to its longer wavelength of 720 nm, contributed by the AuNPs transformation from dispersed to aggregated state respectively is revealed in the UV vis spectrum (Fig 2C). Dynamic light scattering (DLS) data indicated a hydrodynamic diameter for the synthesized AuNPs, averaging 17.23 nm, consistent with previous reports [44]. The Zeta potential of the AuNPs

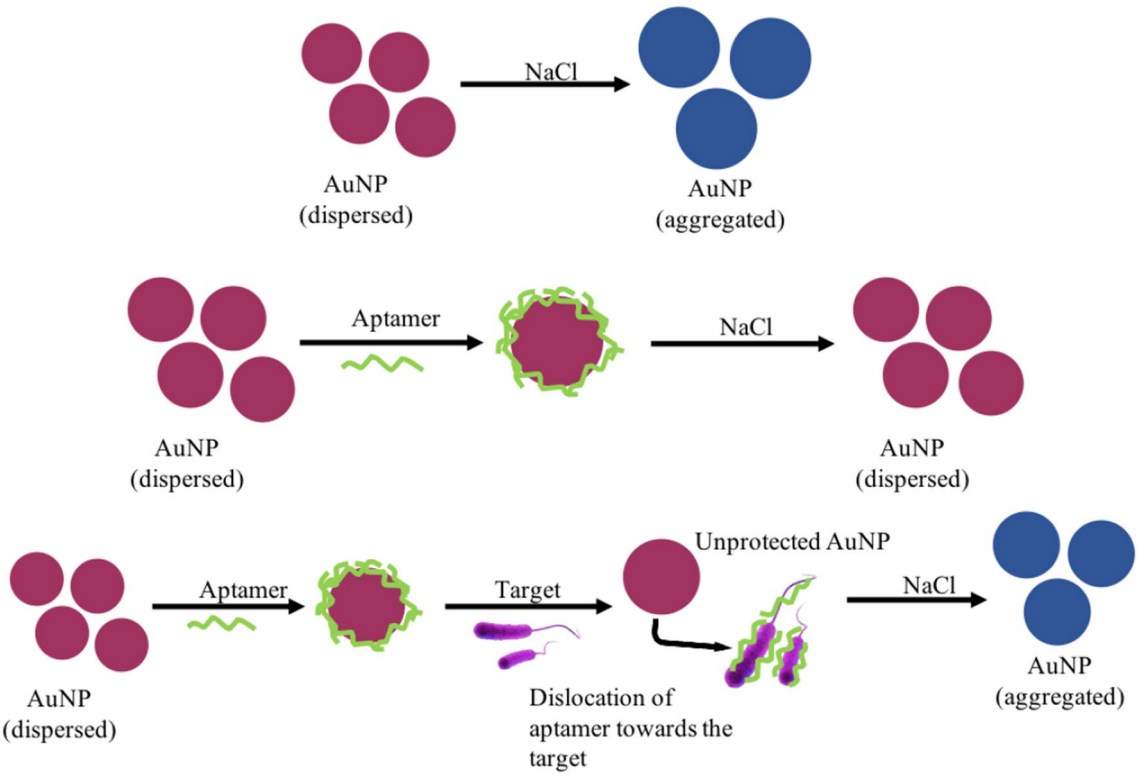

Fig. 1 Schematic illustration of AuNP target detection mechanism

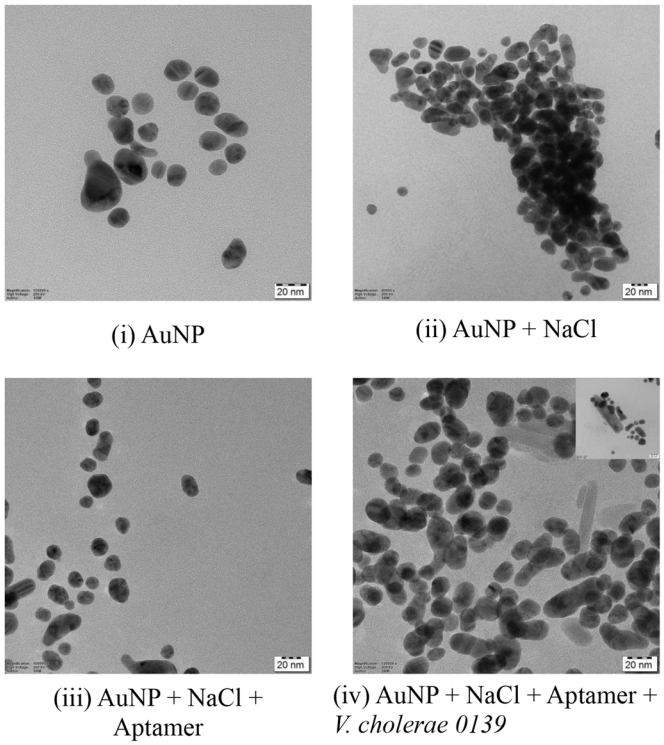

A) Transmission Electron Microscopy images of AuNPs and target detection

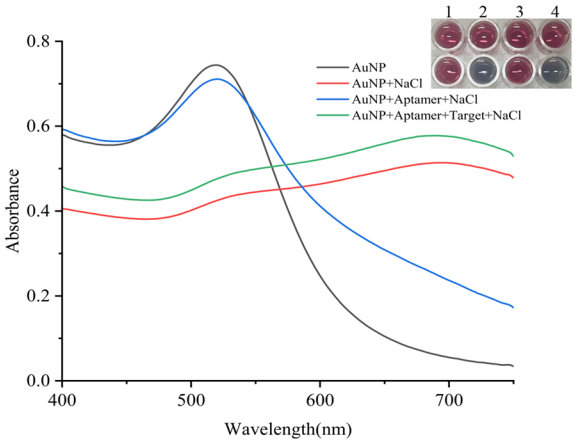

C) UV-visible absorption spectra (1) AuNPs, (2) AuNPs + NaCl (3) AuNPs +Aptamer + NaCl. Inset: color changes observed by naked eyes.

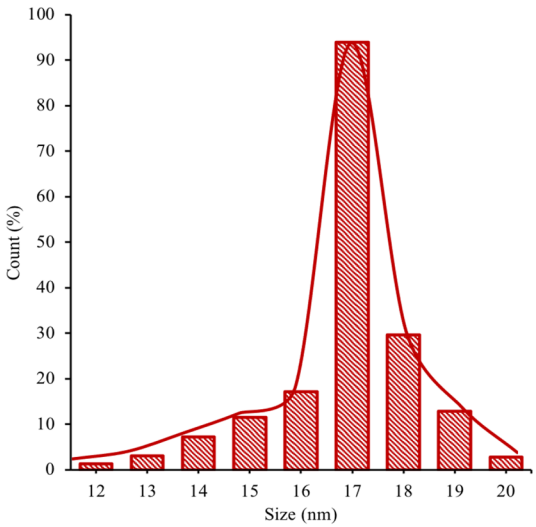

B) Size distribution plot of AuNPs

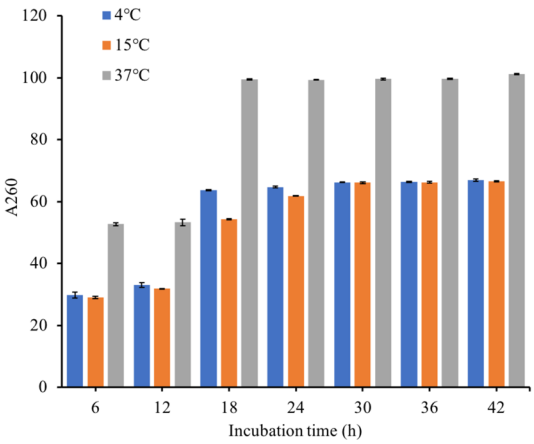

D) Effect of incubation time and reaction temperature on binding rates of the aptamer to AuNPs.

Fig. 2 **A** Transmission electron microscopy images of AuNPs and target detection. **B** Size distribution plot of AuNPs. **C** UV–visible absorption spectra (1) AuNPs, (2) AuNPs + NaCl, (3) AuNPs + Aptamer + NaCl. Inset: color changes observed by naked eyes. **D** Effect of incubation time and reaction temperature on binding rates of the aptamer to AuNPs

was determined to be − 17.9 mV. The conjugation process was facilitated by electric double-layer formation. In this process, the phosphate backbone of the aptamer sequence interacts with the metal surface of the AuNPs, resulting in an elevation of the surface charge to − 24.2 mV in the Apt-AuNPs [45].

For the effective conjugation between aptamer and AuNP, different incubation times and temperatures were tested to

find the optimum condition. The result indicated that the increase in temperature increased conjugation Elevated temperatures have been found to accelerate the process of aptamer binding to AuNPs. Also, the conjugation requires less time at 37 °C in comparison to the lower temperature. At 37 °C, the conjugation saturate after 18 h. Therefore, we have established that the most favorable condition for the creation of an effective aptasensor, while ensuring the integrity of the AuNPs and aptamers, is 18 h at 37 °C (Fig 2D). Ma et al., found that the optimal conditions for conjugation were 37 °C incubation for 24 h, and it is aligned with our study result [46].

Optimization of NaCl and Aptamer Concentrations

The effectiveness of the aptasensor is dependent upon the optimal concentration of NaCl and aptamer. In our experiments, we tested different concentrations of NaCl, ranging from 0.25 to 3 M, and observed a gradual change in color with increasing NaCl concentration. The saturation point was attained at 1 M NaCl concentration; no further changes were seen. This disruption led to the aggregation of the AuNPs, which increased their SPR wavelength from 520 to 720 nm (Fig. 3A).

Determining the ideal concentration of aptamers is crucial in preventing rapid and extensive AuNP aggregation in the optimal NaCl concentrations. To optimize the concentration, varying concentrations of aptamers ranging from 0 to 200 pM were incubated with AuNPs at their optimum temperature and duration (37 °C for 18 h). Subsequently, 1 M of NaCl was added to each sample, and their spectral analysis and color changes were observed. Aggregation of AuNPs was not observed at higher aptamer concentrations (120, 160, and 200 pM), and they retained their ruby red color. However, visible color changes and aggregation were observed at lower NaCl concentrations (Fig. 3B). Despite being in a NaCl environment, Apt-AuNPs showed more excellent stability and reduced salt-induced aggregation as the aptamers protected them [47, 48]. Gold nanoparticles with a high aptamer concentration are more stable, but the residual aptamer concentration or background interference may reduce the detection sensitivity [41]. Therefore, the optimal aptamer concentration was determined to be 120 pM for further experiments.

Sensitivity Assessment of an Aptasensor Towards *Vibrio cholerae* O139

To test the sensitivity of the biosensor, *V. cholerae* O139 was detected at varying concentrations (ranging from 1 to 10^8 CFU/mL) under optimized experimental conditions of 120 pM aptamer and 1 M NaCl. The biosensor used SPR absorbance ratios (A_{720}/A_{520}) to determine AuNP aggregation [49]. As target concentration rose, NaCl triggered AuNPs aggregation, which caused the color to shift from red to purple (as seen in Fig. 4A). This suggests that aptamers bound to *V. cholerae* O139 became dislodged from the surface of AuNPs, allowing for NaCl-triggered

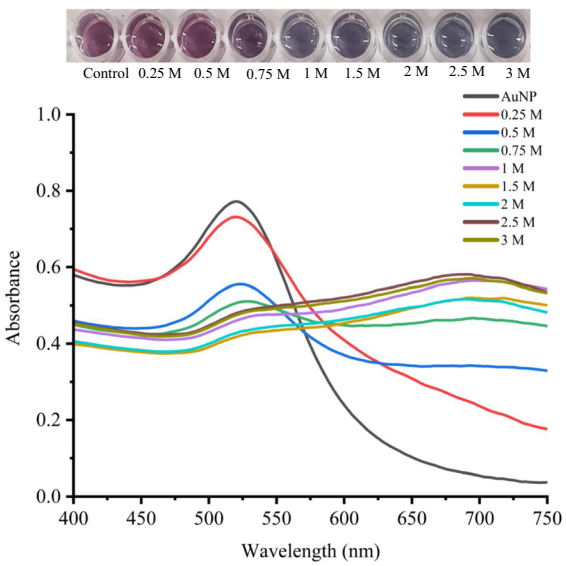

Fig. 3, A) UV-visible absorption spectra showing aggregation of AuNP after the addition of different concentrations of NaCl (0.25 - 3.0 M).

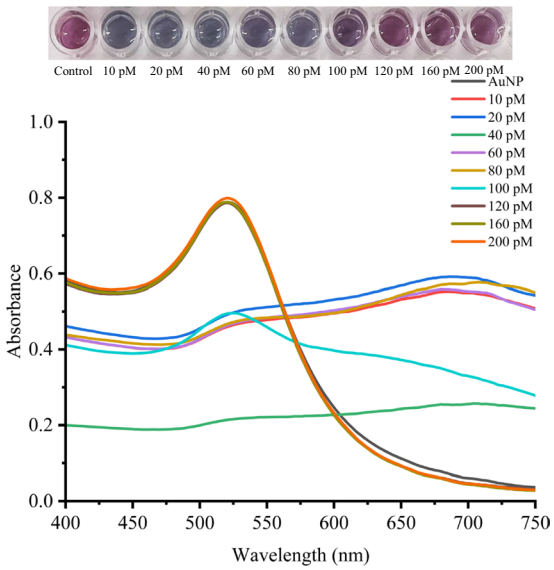

B) UV-visible absorption spectra showing optimizing of aptamer concentrations against NaCl induced aggregation (10 - 200 pM). Inset: color changes observed by naked eyes.

Fig. 3 **A** UV–visible absorption spectra showing aggregation of AuNP after the addition of different concentrations of NaCl (0.25–3.0 M). **B** UV–visible absorption spectra showing optimizing of aptamer concentrations against NaCl induced aggregation (10–200 pM). Inset: color changes observed by naked eyes

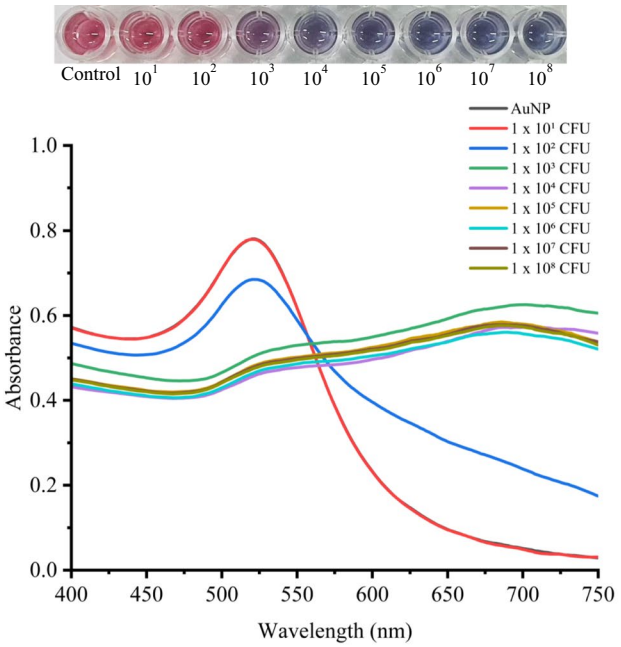

Sensitivity assay: (A) UV-visible absorption spectra showing the detection of *V. cholerae O139* at different concentrations ($1x10^1$ - 10^8 CFU/mL^{-1})

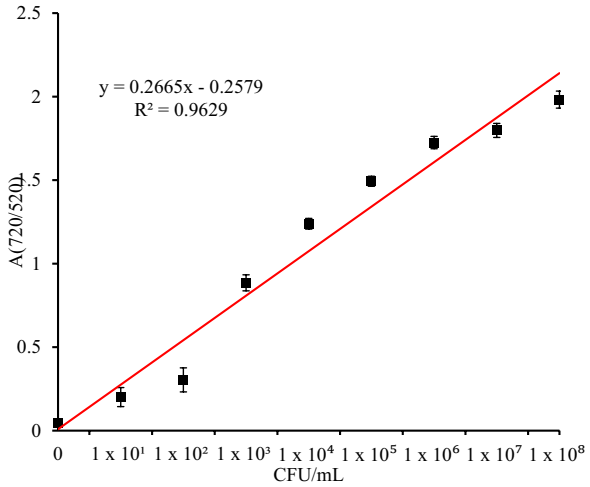

B) The calibration curves of A_{720}/A_{520} ratios versus log of *V. cholerae O139* concentrations.

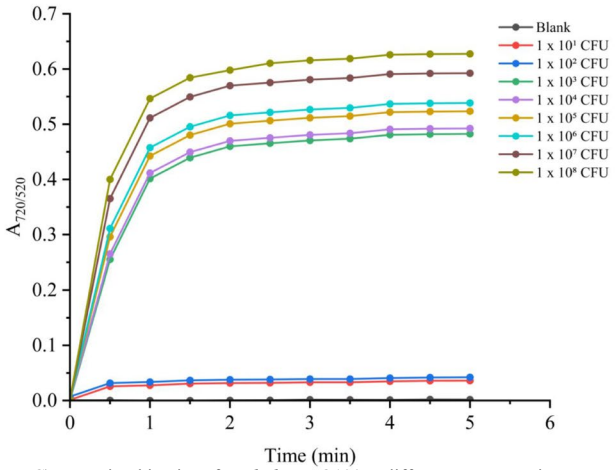

C) Detection kinetics of *V. cholerae O139* at different concentrations ($1x10^1$ - 10^8 CFU mL^{-1}).

Fig. 4 Sensitivity assay: **A** UV–visible absorption spectra showing the detection of *V. cholerae O139* at different concentrations (1×10^1–10^8 CFU/mL^{-1}). **B** The calibration curves of A_{720}/A_{520} ratios versus log of *V. cholerae O139* concentrations. **C** Detection kinetics of *V. cholerae O139* at different concentrations (1×10^1–10^8 CFU/mL)

aggregation. The aptasensor exhibited a linear correlation with target concentration, with a regression equation of $y=0.2665x-0.2579$ ($R^2=0.9629$) (Fig. 4B). The detection limit (LOD) was determined to be 587 ± 2.54 CFU/mL, following the guidelines provided by the International Union of Pure and Applied Chemistry [50].

$$LOD = 3.3\times\sigma/S$$

where σ stands for the response's standard deviation, S stands for the calibration curve slope.

Furthermore, the procedure was quick, and the test results were visible within 2 min, which were then evaluated using detection kinetics at A_{720} (Fig. 4C).

There are very few detection methods currently available that can detect the whole cell of *V. cholera* (Table 1).

Table 1 Various biosensors for the detection of *Vibrio cholera*

Biosensor	Technique	Target	Method	LOD	Detection time	References
Colorimetric	LFA	Cholera toxin	GM-1 aptamer sandwich	10 ng/mL	15 min	[51]
Optical	ELASA	*V. cholerae* O1	Aptamer-nanobody	10^4 CFU/mL	5 h	[52]
Fluorescence	Label-free detection	*V. cholerae* O139	Quantum dot-Aptamer quenching	426 CFU/mL	10 min	[38]
Molecular	Multiplex PCR	*V. cholerae* O139	Micro array	10^3 CFU/mL	3 h	[53]
	Multiplex PCR	*V. cholerae* O139	Reverse transcription	7 CFU/mL	7–8 h	[54]
	Multiplex PCR	*V. cholerae* O139	Capillary electrophoresis	5–20 CFU/mL	8 min	[56]
	Nucleic acid sequence-based amplification (NASBA)	*V. cholerae* O139	Molecular beacons	50 CFU/mL	3 h	[58]
	LAMP PCR	*V. cholerae* O139	Precipitation	7.8/10^2 CFU/g	70 min	[55]
LFD and RDT	Dot-blot ELISA	*V. cholerae* O139	Serological assay (Mab)	10^5–10^7 CFU/mL	90 min	[57]
	Sensitive membrane antigen rapid test (SMART)	*V. cholerae* O139	Serological assay (Mab)	6×10^7 CFU/mL	15 min	[59, 60]
	Bengal screen test	*V. cholerae* O139	Anti *V. cholerae* O139 antigen	2×10^3 CFU/mL	5 min	[61]
	Immuno-chromatography	*V. cholerae* O139	Anti *V. cholerae* O139 antigen	1×10^6 CFU/mL	5 min	[9]
Colorimetric	Salt induced aggregation	*V. cholerae* O139	AuNP-NaCl aggregation	614 CFU/mL	2 min	This method

Frohnmeyer et al. developed a colorimetric lateral flow test that detects cholera toxin with the LOD of 10 ng/mL, enhancing sensitivity with GM1-functionalized liposomes and aptamers [51]. An optical ELASA procedure utilized VHHs and biotinylated aptamers for *V. cholerae* O1 detection at 10^4 CFU/mL [52]. Our previous study developed a label-free fluorescent biosensor using quantum dots to detect *V. cholerae* O139, with a detection limit of 426 CFU/mL [38]. Similarly molecular methods such as, multiplex PCR with tyramide signal amplification identified various diseases including *V. cholerae* O139 [53], several sensitive assays were developed, including RT-PCR [54], capillary electrophoresis [55], molecular beacon-based NASBA [56], LAMP assay [57] for the sensitive detection of *V. cholera*.

Our aptasensor has better LOD than the ELISA and other biosensors except nucleic acid amplification methods. However, most of these techniques require trained personnel, sophisticated machinery, and methods that make the detection crucial.

Our AuNP-based biosensor is cheaper than the other reported methods for detecting *V. cholera* O139 because neither the aptamers nor AuNP are modified. Our method also has a detection time almost superior to that of the existing biosensors. Furthermore, our proposed method does not require any specific instruments or workforce for implementation, and it can be easily converted into a point-of-care device for the screening of environmental and clinical samples for the presence of the target pathogen.

Evaluating the Selectivity of Developed Aptasensor

The specificity of the aptasensor was determined by analyzing its detection capabilities in multiple non-target bacteria, including *V. parahaemolyticus*, *S. aureus*, *A. hydrophila*, and *E. coli*. The aptamer did not bind to the non-target bacteria or detach them from the surface of AuNPs. As a result, no noticeable color change was observed upon adding NaCl. However, a color change was observed in the presence of the target bacterium, *V. cholerae* O139 (Fig. 5A). Although closely related species (*V. parahaemolyticus* and *V. vulnificus*) and common waterborne pathogens (*MRSA* and *E. coli*) were tested, the results showed that aggregation only occurred in the presence of the target organism (Fig. 5B). Additionally, detection kinetics were performed to determine the time taken for the biosensor to detect its target organism. Each sample's spectral data was taken every 30 s until the end of the aggregation reaction.

These findings demonstrated that this colorimetric aptasensor has a high selectivity for its target *V. cholerae* O139. Similarly, a lateral flow assay, aptamer-AuNP, detected the GM1 cholera toxin receptor with a 10 ng/mL LOD [51].

Detection of *V. cholerae* O139 in the Environmental Sample

The effectiveness of the AuNP aptasensor in detecting *V. cholerae* in lake water was evaluated through recovery studies O139. Colorimetric signals in water samples

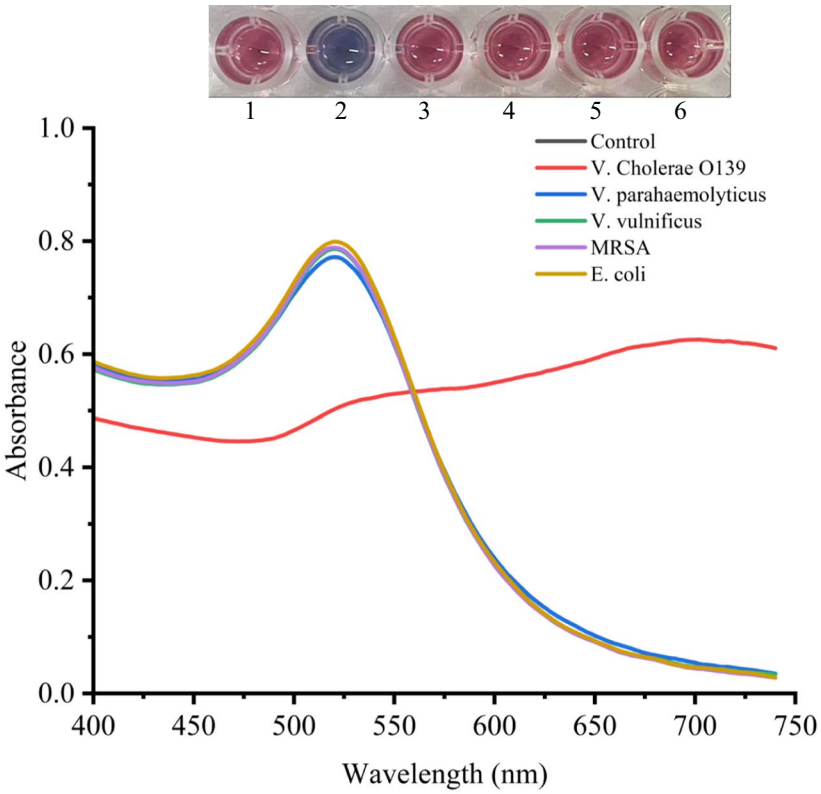

Fig. 5 Selectivity assay: **A** UV–visible absorption spectra showing specific detection of (1) *V. cholerae O139* among different non-target bacterium, (2) *V. parahaemolyticus*, (3) *V. vulnificus*, (4) *MRSA*, and (5) *E. coli*. **B** Detection kinetics of *V. cholerae O139* with non-target bacterium *V. parahaemolyticus*, *V. vulnificus*, *MRSA*, and *E. coli* (10^6 CFU/mL^{-1})

Selectivity assay: A) UV-visible absorption spectra showing specific detection of 1) *V. cholerae O139* among different non-target bacterium 2) *V. parahaemolyticus,* 3) *V, vulnificus,* 4) *MRSA, and* 5) *E. coli*

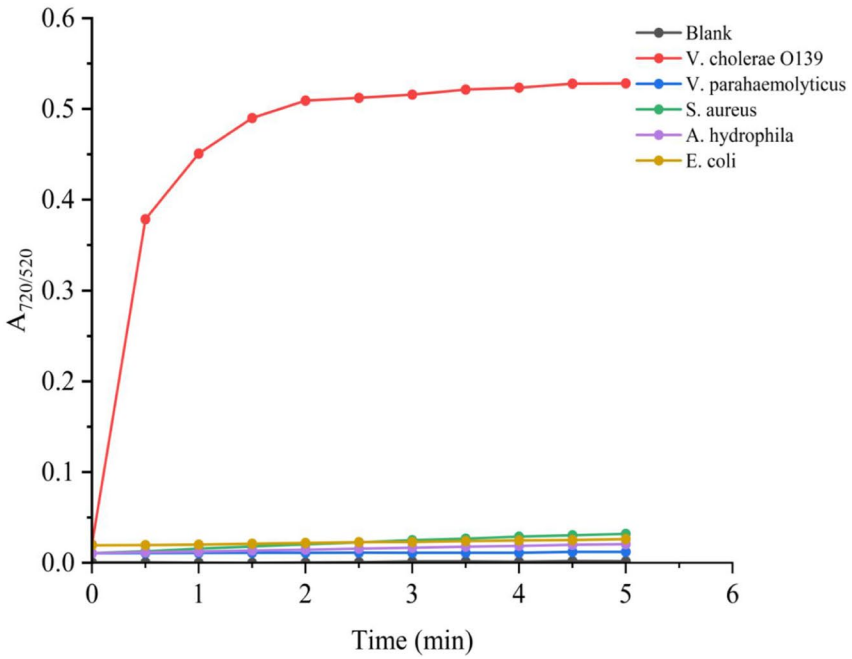

B) Detection kinetics of *V. cholerae O139* with non-target bacterium *V. parahaemolyticus, V, vulnificus, MRSA, and E. coli* (10^6 CFU/mL^{-1}).

Table 2 Recovery studies using real samples

Sample	Spiked (CFU/mL)	Measured (CFU/mL)	Recovery of the assay (%)	RSD (%) (n = 3)
1	0	0	0	0
2	5×10^2	3.7×10^2	74.2	4.48
3	1×10^3	0.87×10^3	87.9	3.61
4	5×10^3	0.42×10^4	85.8	2.02
5	1×10^4	0.86×10^4	86.2	1.75
6	5×10^4	0.42×10^5	85.5	0.34

containing *V. cholerae* were measured using $A_{720/520}$ O139. The samples' results, recoveries, and relative standard deviation (RSD) are outlined in Table 2. The test recoveries of the lake water range from 74.2 to 85.5%, with RSD values ranging from 0.34 to 4.48%. This indicates that the method is highly replicable in actual samples when identifying *V. cholerae* O139. Therefore, this method is reliable for detecting *V. cholerae* O139 in real samples.

Development of Aptasensor in Paper-Based Platform

The paper-based biosensor plays a crucial role in developing point-of-care devices for pathogen detection, owing to its convenience in storage and transportation. We have functionally analyzed the developed biosensor on the paper-based platform. The Whatman paper discs (detection and control) were added with Apt-AuNPs complex (10 µL) and allowed for complete diffusion over the entire surface of the disc. Then, *V. cholerae* O139 cells are loaded in each well and incubated for 2 min at the detection disc with *V. cholerae* O139 caused aggregation leads to a change in color of the disc from ruby red to blue color, while the disc without the target AuNP-aptamer complex remains unchanged in the control disc (Fig. 6A). A picture of discs were captured using a smartphone. Its RGB values were calculated using ImageJ software. The results showed that the disc with target showed a noticeable RGB value shift than the control discs (Fig. 6B). This phenomenon is due to the binding of aptamer with its target pathogen with a higher affinity that enhanced the dislocation of aptamer from the AuNPs surface towards the surface of *V. cholerae* O139 and make the disc change its color from ruby red.

This work developed a simple and label-free strategy to detect *V. cholerae* without requiring expensive machinery. The process takes only 2 min, and the result is distinguishable to the naked eye. The method uses only a few simple chemicals and reagents, reducing the overall detection cost. The chosen aptamer is highly selective for *V. cholerae*, ensuring accurate detection. The AuNPs-Aptamer complex is loaded onto paper discs, and color changes can be observed without needing additional equipment. This AuNP-Aptamer-based biosensor is highly effective in detecting *V. cholerae* organisms in suspectable environments O139.

Conclusion

Cholera is the most common waterborne disease that affects public health worldwide. Although traditional molecular techniques are both specific and sensitive, they are not appropriate for quick on-site testing. In this study, we explored the colorimetric detection of *V. cholerae* O139 using an aptasensor. The aptamers coated on the surface of AuNPs can inhibit AuNPs from aggregating when exposed to NaCl since *V. cholerae* bind to aptamers more preferentially than AuNPs. The solution's color changes paralleled the changes in *V. cholerae* concentration in the range of 10^3 to 10^8 CFU/mL, exhibiting an excellent linear correlation with a limit of detection of 587 CFU/mL. This detection system takes only 2 min to complete and works well in environmental sample detection. It is thus highly compatible with on-site testing and has advantages over traditional bacterial culture and other molecular detection techniques. Additionally, this aptasensor directly detects the whole pathogen, and the results are observable to the human eye, eliminating the need for laborious processes like DNA extraction and purification. Furthermore, a simple paper-based detection method was also developed, which can be used as an alternative tool for on-field detection of *V. cholerae*.

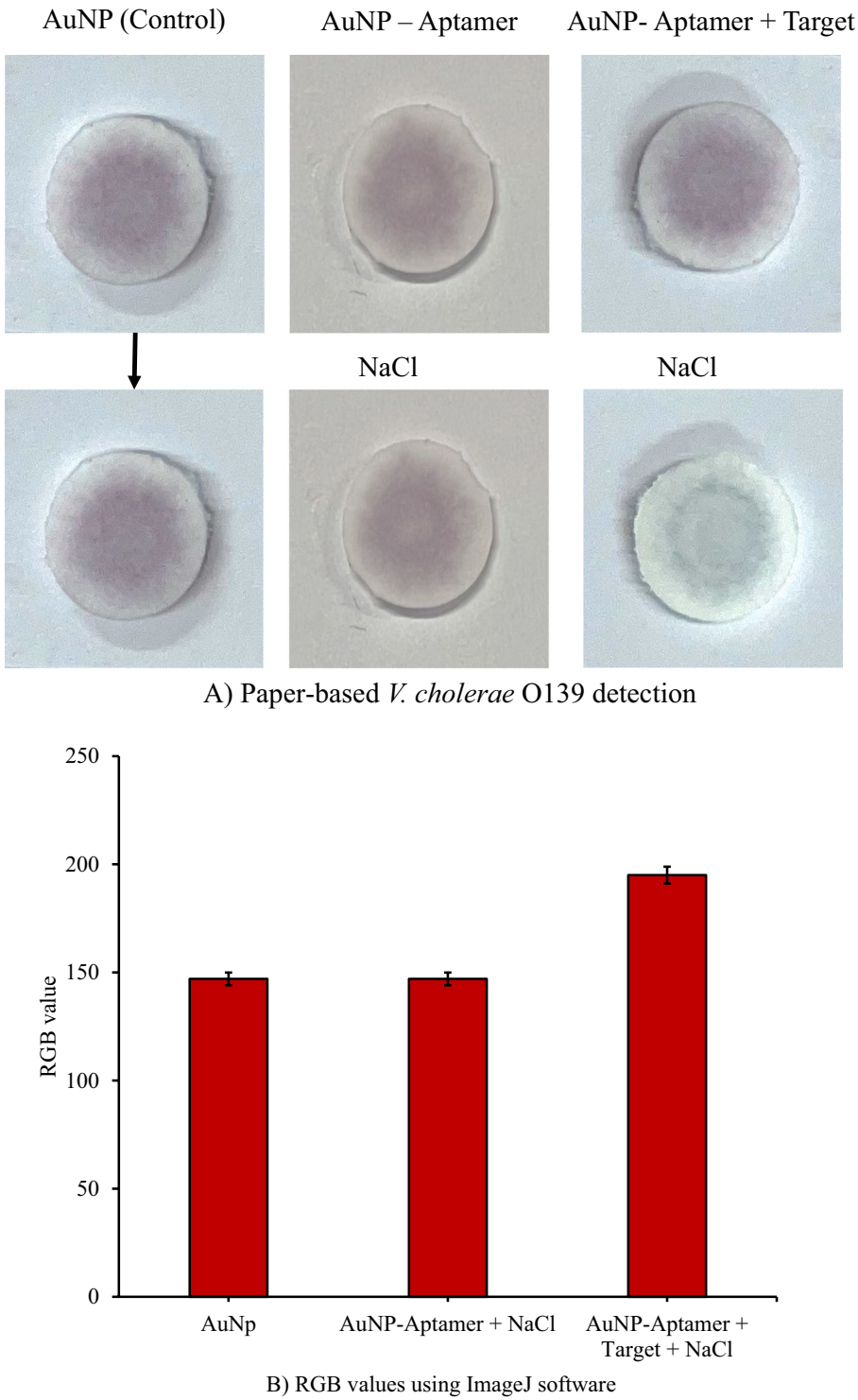

Fig. 6 **A** Paper-based *V. cholerae* O139 detection. **B** RGB values using ImageJ software

Acknowledgments We thank the SRM Institute of Science and Technology for their financial support of the project.

Author Contributions Masilamani Karthikeyan: methodology, investigation, writing; Pasupathi Rathinasabapathi: conceptualization, supervision, writing—original draft, writing—review & editing, resources, funding acquisition.

Data Availability The datasets used and/or analysed during the current study are available from the corresponding author upon reasonable request.

Declarations

Competing Interests The authors declare that they have no competing interests.

Ethical Approval This article contains no studies with human participants and animals performed by authors.

References:

1. Ghosh-Banerjee, J., M. Senoh, T. Takahashi, T. Hamabata, S. Barman, H. Koley, et al. Cholera toxin production by the El Tor variant of *Vibrio cholerae* O1 compared to prototype El Tor and classical biotypes. *J. Clin. Microbiol.* 48:4283–4286, 2010.
2. Nelson, E. J., J. B. Harris, J. G. Morris, S. B. Calderwood, and A. Camilli. Cholera transmission: the host, pathogen and bacteriophage dynamic. *Nat. Rev. Microbiol.* 7:693–702, 2009.
3. Chatterjee, P., S. Kanungo, S. K. Bhattacharya, and S. Dutta. Mapping cholera outbreaks and antibiotic resistant *Vibrio cholerae* in India: an assessment of existing data and a scoping review of the literature. *Vaccine*. 38(Suppl 1):A93-104, 2020.
4. Alam, M., N. A. Hasan, M. Sultana, G. B. Nair, A. Sadique, A. S. G. Faruque, et al. Diagnostic limitations to accurate diagnosis of cholera. *J. Clin. Microbiol.* 48:3918–3922, 2010.
5. Cooper, K. L. F., C. K. Y. Luey, M. Bird, J. Terajima, G. B. Nair, K. M. Kam, et al. Development and validation of a PulseNet standardized pulsed-field gel electrophoresis protocol for subtyping of *Vibrio cholerae*. *Foodborne Pathog. Dis.* 3:51–58, 2006.
6. Yu, C. Y., G. Y. Ang, A. L. Chua, E. H. Tan, S. Y. Lee, G. Falero-Diaz, et al. Dry-reagent gold nanoparticle-based lateral flow biosensor for the simultaneous detection of *Vibrio cholerae* serogroups O1 and O139. *J. Microbiol. Methods*. 86:277–282, 2011.
7. Ramamurthy, T., S. K. Bhattacharya, Y. Uesaka, K. Horigome, M. Paul, D. Sen, et al. Evaluation of the bead enzyme-linked immunosorbent assay for detection of cholera toxin directly from stool specimens. *J. Clin. Microbiol.* 30:1783–1786, 1992.
8. Goel, A. K., S. Ponmariappan, D. V. Kamboj, and L. Singh. Single multiplex polymerase chain reaction for environmental surveillance of toxigenic-pathogenic O1 and non-O1 *Vibrio cholerae*. *Folia Microbiol. (Praha)*. 52:81–85, 2007.
9. Thattiyaphong, A., K. Okada, S. Khangrang, W. Nispa, P. Sawanpanyalert, and T. Honda. Development of a 5-minute rapid test for detecting *Vibrio cholerae* O139. *Southeast Asian J. Trop. Med. Public Health*. 44:448–455, 2013.
10. Huq, A., B. J. Haley, E. Taviani, A. Chen, N. A. Hasan, and R. R. Colwell. Detection, isolation, and identification of *Vibrio cholerae* from the environment. *Curr. Protoc. Microbiol.* Chapter 6:Unit6A.5, 2012.
11. Byun, J. Recent progress and opportunities for nucleic acid aptamers. *Life (Basel)*. 11:193, 2021.
12. Zhao, Y.-W., H.-X. Wang, G.-C. Jia, and Z. Li. Application of aptamer-based biosensor for rapid detection of pathogenic *Escherichia coli*. *Sensors (Basel)*. 18:2518, 2018.
13. Van Dorst, B., J. Mehta, K. Bekaert, E. Rouah-Martin, W. De Coen, P. Dubruel, et al. Recent advances in recognition elements of food and environmental biosensors: a review. *Biosens. Bioelectron.* 26:1178–1194, 2010.
14. Kim, Y. S., N. H. A. Raston, and M. B. Gu. Aptamer-based nanobiosensors. *Biosens. Bioelectron.* 76:2–19, 2016.
15. Jain, P. K., X. Huang, I. H. El-Sayed, and M. A. El-Sayed. Review of some interesting surface plasmon resonance-enhanced properties of noble metal nanoparticles and their applications to biosystems. *Plasmonics*. 2:107–118, 2007. https://doi.org/10.1007/s11468-007-9031-1.
16. Ye, H., K. Yang, J. Tao, Y. Liu, Q. Zhang, S. Habibi, et al. An enzyme-free signal amplification technique for ultrasensitive colorimetric assay of disease biomarkers. *ACS Nano.* 11:2052–2059, 2017.
17. Crivianu-Gaita, V., and M. Thompson. Aptamers, antibody scFv, and antibody Fab' fragments: an overview and comparison of three of the most versatile biosensor biorecognition elements. *Biosens. Bioelectron.* 85:32–45, 2016.
18. Huang, R., N. He, and Z. Li. Recent progresses in DNA nanostructure-based biosensors for detection of tumor markers. *Biosens. Bioelectron.* 109:27–34, 2018.
19. Wu, W., J. Li, D. Pan, J. Li, S. Song, M. Rong, et al. Gold nanoparticle-based enzyme-linked antibody-aptamer sandwich assay for detection of *Salmonella* Typhimurium. *ACS Appl. Mater. Interfaces*. 6:16974–16981, 2014.
20. Wu, S., Y. Wang, N. Duan, H. Ma, and Z. Wang. Colorimetric aptasensor based on enzyme for the detection of *Vibrio parahemolyticus*. *J. Agric. Food Chem.* 63:7849–7854, 2015.
21. Wu, W., S. Zhao, Y. Mao, Z. Fang, X. Lu, and L. Zeng. A sensitive lateral flow biosensor for *Escherichia coli* O157:H7 detection based on aptamer mediated strand displacement amplification. *Anal. Chim. Acta*. 861:62–68, 2015.
22. Chang, T., L. Wang, K. Zhao, Y. Ge, M. He, and G. Li. Duplex identification of *Staphylococcus aureus* by aptamer and gold nanoparticles. *J. Nanosci. Nanotechnol.* 16:5513–5519, 2016.
23. Bayraç, C., F. Eyidoğan, and H. Avni Öktem. DNA aptamer-based colorimetric detection platform for *Salmonella enteritidis*. *Biosens. Bioelectron.* 98:22–28, 2017.
24. Dehghani, Z., M. Hosseini, J. Mohammadnejad, B. Bakhshi, and A. H. Rezayan. Colorimetric aptasensor for *Campylobacter jejuni* cells by exploiting the peroxidase like activity of Au@Pd nanoparticles. *Mikrochim. Acta*. 185:448, 2018.
25. Kim, Y.-J., H.-S. Kim, J.-W. Chon, D.-H. Kim, J.-Y. Hyeon, and K.-H. Seo. New colorimetric aptasensor for rapid on-site detection of *Campylobacter jejuni* and *Campylobacter coli* in chicken carcass samples. *Anal. Chim. Acta*. 1029:78–85, 2018.
26. Liu, Y., J. Wang, X. Song, K. Xu, H. Chen, C. Zhao, et al. Colorimetric immunoassay for *Listeria monocytogenes* by using core gold nanoparticles, silver nanoclusters as oxidase mimetics, and aptamer-conjugated magnetic nanoparticles. *Mikrochim. Acta*. 185:360, 2018.
27. Zhu, W., Z. Li, X. Liu, X. Yan, and L. Deng. Determination of *Shigella flexneri* by a novel fluorescent aptasensor. *Anal. Lett.* 48:2870–2881, 2015. https://doi.org/10.1080/00032719.2015.1052974.
28. Wang, J., J. L. Davidson, S. Kaur, A. A. Dextre, M. Ranjbaran, M. S. Kamel, et al. Paper-based biosensors for the detection of nucleic acids from pathogens. *Biosensors (Basel)*. 12:1094, 2022.
29. Tang, D., J. Tang, B. Su, J. Ren, and G. Chen. Simultaneous determination of five-type hepatitis virus antigens in 5 min using an integrated automatic electrochemical immunosensor array. *Biosens. Bioelectron.* 25:1658–1662, 2010.
30. Qiao, J., Y.-H. Hwang, C.-F. Chen, L. Qi, P. Dong, X.-Y. Mu, et al. Ratiometric fluorescent polymeric thermometer for thermogenesis investigation in living cells. *Anal. Chem.* 87:10535–10541, 2015. https://doi.org/10.1021/acs.analchem.5b02791.
31. Tripathy, S. K., J. Y. Woo, and C.-S. Han. Surface-plasmon-based colorimetric detection of Cu(II) ions using label-free gold nanoparticles in aqueous thiosulfate systems. *Nanotechnology*.23:305502, 2012. https://doi.org/10.1088/0957-4484/23/30/305502.
32. Zhou, J., C. Zhang, and Y. Wang. Nanoporous block copolymer membranes immobilized with gold nanoparticles for continuous flow catalysis. *Polym. Chem.* 10:1642–1649, 2019.

33. Kim, K., Y.-S. Nam, Y. Lee, and K.-B. Lee. Highly sensitive colorimetric assay for determining Fe^{3+} based on gold nanoparticles conjugated with glycol chitosan. *J. Anal. Methods Chem.* 2017:3648564, 2017.
34. López-Marzo, A. M., and A. Merkoçi. Paper-based sensors and assays: a success of the engineering design and the convergence of knowledge areas. *Lab Chip*. 16:3150–3176, 2016.
35. Chen, N., H. Liu, Y. Zhang, Z. Zhou, W. Fan, G. Yu, et al. A colorimetric sensor based on citrate-stabilized AuNPs for rapid pesticide residue detection of terbuthylazine and dimethoate. *Sens. Actuators B*. 255:3093–3101, 2018.
36. Liu, X., M. Atwater, J. Wang, and Q. Huo. Extinction coefficient of gold nanoparticles with different sizes and different capping ligands. *Colloids Surf. B*. 58:3–7, 2007.
37. Xu, Z., X. Bi, Y. Huang, Z. Che, X. Chen, M. Fu, et al. Sensitive colorimetric detection of *Salmonella enteric* serovar typhimurium based on a gold nanoparticle conjugated bifunctional oligonucleotide probe and aptamer. *J. Food Saf.* 38:e12482, 2018. https://doi.org/10.1111/jfs.12482.
38. Karthikeyan, M., G. D. Venkatasubbu, and P. Rathinasabapathi. A label-free carbon dots-based fluorescent aptasensor for the detection of *V. cholerae* O139. *Diam. Relat. Mater.* 137:110173, 2023.
39. Zhang, Y., D. Gao, J. Fan, J. Nie, S. Le, W. Zhu, et al. Naked-eye quantitative aptamer-based assay on paper device. *Biosens. Bioelectron.* 78:538–546, 2016.
40. Zoghi, S., and M. Rahmandoust. A novel technique to overcome fluid flow influence in carbon quantum dots/paper-based analytical devices. *Sci. Rep.* 12:17861, 2022.
41. Ma, Q., Y. Wang, J. Jia, and Y. Xiang. Colorimetric aptasensors for determination of tobramycin in milk and chicken eggs based on DNA and gold nanoparticles. *Food Chem.* 249:98–103, 2018.
42. Zhao, W., M. A. Brook, and Y. Li. Design of gold nanoparticle-based colorimetric biosensing assays. *ChemBioChem*. 9:2363–2371, 2008.
43. Lavu, P. S. R., B. Mondal, S. Ramlal, H. S. Murali, and H. V. Batra. Selection and characterization of aptamers using a modified whole cell bacterium SELEX for the detection of *Salmonella enterica* serovar typhimurium. *ACS Comb. Sci.* 18:292–301, 2016.
44. Das, R., A. Dhiman, A. Kapil, V. Bansal, and T. K. Sharma. Aptamer-mediated colorimetric and electrochemical detection of *Pseudomonas aeruginosa* utilizing peroxidase-mimic activity of gold NanoZyme. *Anal. Bioanal. Chem.* 411:1229–1238, 2019.
45. Alsager, O. A., K. M. Alotaibi, A. M. Alswieleh, and B. J. Alyamani. Colorimetric aptasensor of vitamin D3: a novel approach to eliminate residual adhesion between aptamers and gold nanoparticles. *Sci. Rep.* 8:12947, 2018.
46. Ma, X., L. Song, N. Zhou, Y. Xia, and Z. Wang. A novel aptasensor for the colorimetric detection of *S. typhimurium* based on gold nanoparticles. *Int. J. Food Microbiol.* 245:1–5, 2017.
47. Verma, M. S., J. L. Rogowski, L. Jones, and F. X. Gu. Colorimetric biosensing of pathogens using gold nanoparticles. *Biotechnol. Adv.* 33:666–680, 2015.
48. Wang, L., X. Liu, X. Hu, S. Song, and C. Fan. Unmodified gold nanoparticles as a colorimetric probe for potassium DNA aptamers. *Chem. Commun. (Camb.)*. 36:3780–3782, 2006.
49. Schmitz, F. R. W., K. Cesca, A. Valério, D. de Oliveira, and D. Hotza. Colorimetric detection of *Pseudomonas aeruginosa* by aptamer-functionalized gold nanoparticles. *Appl. Microbiol. Biotechnol.* 107:71–80, 2023.
50. Moabelo, K. L., T. M. Lerga, M. Jauset-Rubio, N. R. S. Sibuyi, C. K. O'Sullivan, M. Meyer, et al. A label-free gold nanoparticles-based optical aptasensor for the detection of retinol binding protein 4. *Biosensors*. 12:1061, 2022.
51. Frohnmeyer, E., N. Tuschel, T. Sitz, C. Hermann, G. T. Dahl, F. Schulz, et al. Aptamer lateral flow assays for rapid and sensitive detection of cholera toxin. *Analyst*. 144:1840–1849, 2019.
52. Mojarad, A. E., and S. L. M. Gargaria. Aptamer-nanobody based ELASA for detection of *Vibrio cholerae* O1. *Iran. J. Microbiol.* 12:263–272, 2020.
53. Jin, D., H. Qi, S. Chen, T. Zeng, Q. Liu, and S. Wang. Simultaneous detection of six human diarrheal pathogens by using DNA microarray combined with tyramide signal amplification. *J. Microbiol. Methods*. 75:365–368, 2008.
54. Kanoktippornchai, B., C. Chomvarin, C. Engchanil, and W. Wongboot. Triplex reverse transcription-PCR for detecting viable toxigenic *Vibrio cholerae* in water samples in Thailand. *Southeast Asian J. Trop. Med. Public Health*. 45:375–382, 2014.
55. Yamazaki, W. Sensitive and rapid detection of cholera toxin-producing *Vibrio cholerae* using loop-mediated isothermal amplification. *Methods Mol. Biol.* 739:13–22, 2011.
56. Zhou, C., M. Li, C. Sun, H. Zou, X. Wu, L. Zhang, et al. Identification of *Vibrio cholerae* serotypes in high-risk marine products with non-gel sieving capillary electrophoresis. *Anal. Biochem.* 494:68–75, 2016.
57. Chaicumpa, W., P. Srimanote, Y. Sakolvaree, T. Kalampaheti, M. Chongsa-Nguan, P. Tapchaisri, et al. Rapid diagnosis of cholera caused by *Vibrio cholerae* O139. *J. Clin. Microbiol.* 36:3595–3600, 1998.
58. Fykse, E. M., G. Skogan, W. Davies, J. S. Olsen, and J. M. Blatny. Detection of *Vibrio cholerae* by real-time nucleic acid sequence-based amplification. *Appl. Environ. Microbiol.* 73:1457–1466, 2007.
59. Qadri, F., J. A. Hasan, J. Hossain, A. Chowdhury, Y. A. Begum, T. Azim, et al. Evaluation of the monoclonal antibody-based kit Bengal SMART for rapid detection of *Vibrio cholerae* O139 synonym Bengal in stool samples. *J. Clin. Microbiol.* 33:732–734, 1995.
60. Martinez-Pino, I., F. J. Luquero, K. Sakoba, S. Sylla, M. Haile, R. F. Grais, et al. Use of a cholera rapid diagnostic test during a mass vaccination campaign in response to an epidemic in Guinea, 2012. *PLoS Negl. Trop. Dis.*7:e2366, 2013.
61. Hasan, J. A., A. Huq, G. B. Nair, S. Garg, A. K. Mukhopadhyay, L. Loomis, et al. Development and testing of monoclonal antibody-based rapid immunodiagnostic test kits for direct detection of *Vibrio cholerae* O139 synonym Bengal. *J. Clin. Microbiol.* 33:2935–2939, 1995.